Journal of Computational Physics **181,** 564–576 (2002)
doi:10.1006/jcph.2002.7142

Highly Convergent Simulations of Transport Dynamics in Organic Light-Emitting Diodes

J. C. deMello

Centre for Electronic Materials and Devices, Imperial College, Exhibition Road, South Kensington, London, SW7 2AY, United Kingdom
E-mail: j.demello@ic.ac.uk

Received August 1, 2001; revised May 31, 2002

We present a method-of-lines solution procedure for modelling charge transport and recombination in organic light-emitting diodes operating in the trap-free space-charge-limited regime. The numerical procedure employs a spatial remeshing algorithm based on equidistribution principles as reported by Sanz-Serna and Christie (1986, *J. Comput. Phys.* **67**, 348) and incorporates additional refinements proposed by Revilla (1986, *Int. J. Numer. Methods Eng.* **23**, 2263) and Saucez *et al.* (1996, *J. Comput. Phys.* **128**, 274). The method, which does not give rise to ill-conditioned series of differential equations, offers rapid convergence to the steady state and is especially well suited to systems of equations displaying steep moving solution fronts. The technique is readily extended to more complex systems.

Key Words: organic; polymer; electroluminescence; simulation; drift; diffusion; method of lines; transport; PPV.

INTRODUCTION

Molecular semiconductors have been attracting considerable scientific and commercial interest owing to their potential application in a wide range of electronic devices, including light-emitting diodes (LEDs), solar cells, and thin-film transistors [1]. There has been considerable progress in the development of molecular devices over the past 10 years with, for example, organic LEDs now entering the marketplace as viable contenders to existing inorganic technologies [1]. To some extent, however, attempts to optimise the efficiencies and performance of molecular devices have been hindered by the relative absence of detailed theoretical models describing device behaviour. As with inorganic devices, the injection, transport, and recombination dynamics of charge carriers in organic devices are governed by series of highly nonlinear coupled differential equations. In general these equations are found to be algebraically intractable, and consequently there is considerable interest in the development of effective numerical algorithms for their solution.

0021-9991/02 $35.00

Although a number of commercial software packages are available for simulating transport processes, these have generally been developed for inorganic device materials such as Si and GaAs. Organic semiconductors differ considerably from their inorganic counterparts, exhibiting for example very low carrier mobilities ($\sim 10^{-10}$ m^2 V^{-1} s^{-1}), low relative permittivities ($\sim$3.5), and long recombination times (rate constants for electron–hole recombination $\sim 10^{-18}$ m^3 s^{-1}). An important consequence is that space-charge effects are typically more pronounced in organic devices—it is easier to accumulate regions of excess electronic space-charge in the semiconductor bulk—and hence the concentrations of the charge carriers vary more rapidly in space. These features create difficulties for most commercial packages and as a result many researchers have elected to develop their own algorithms for modelling organic devices. Notable work in this area has for example been reported by Torpey [2], Tessler [3], and the groups of Bassler [4], Friend [5], and Scott [6]. Details of the methodologies used by these researchers are somewhat scarce. However, most have used either the *method of lines* (MOL) or relaxation techniques to infer the steady-state dynamics of operational devices, in which the coupled differential equations are approximated by a series of simultaneous finite-difference equations, evaluated on a uniform, fixed grid. We refer to this technique as the uniform grid method (UGM).

Although the effectiveness of the MOL approach has been successfully demonstrated by the aforementioned researchers, it is nevertheless the case that the use of a fixed grid of uniform data points is computationally inefficient [7]. This is particularly true for systems of evolutionary partial differential equations with solutions displaying steep moving fronts, because a large number of data points (or nodes) must be used to obtain an adequate solution. An obvious example in the field of molecular semiconductors is the light-emitting electrochemical cell where the accumulation of uncompensated mobile ionic charge in the vicinity of the two electrodes creates exceptionally high electric fields [8–10]. However, even for the comparatively simple case of a conventional trap-free space-charge-limited organic light-emitting diode, the fixed-grid MOL approach is computationally wasteful, and significant efficiency gains may be obtained by switching to an adaptive grid methodology. These limitations have previously been noted by Malliaras and Scott, who reported that their use of a uniform grid prevented them from investigating the behaviour of LEDs operating under conditions of high carrier injection; the charge density inside the device varied too rapidly to be accurately digitised with a grid comprising 200 uniformly spaced grid points [6].

The MOL procedure just outlined may be refined by replacing the uniform grid with an adaptive mesh that responds to the evolving shape of the solution profile. Two types of adaptation algorithm may be envisaged: dynamic remeshing, in which the grid is updated continuously as the solution evolves, and static remeshing, in which the grid is updated at discrete time intervals. In dynamic techniques, the nodes generally move according to ordinary differential equations (ODEs) coupled to the problem equations. This often gives rise to ill-conditioned sets of differential equations, which is particularly undesirable in the present application as Poisson's equation itself is liable to create problems of ill-conditioning before the adaptation procedure is even considered.

In this paper we instead employ a *static* spatial remeshing method (SRM) based on equidistribution of an appropriate functional, as previously reported by Revilla [7]. In essence the system of differential equations is allowed to evolve in time according to the standard MOL procedure but the grid is periodically recalculated to ensure that the grid points are primarily concentrated in the spatial regions where the solution is rapidly

changing. A notable advantage of the static SRM is that the remeshing algorithm is independent of the system of equations under study, and hence it may be reused without change to investigate additional problems. Furthermore, as reported by Wouver *et al.*, static methods are highly competitive with more complex problem-specific dynamic remeshing algorithms and, importantly, do *not* give rise to ill-conditioned sets of differential equations [11].

Wouver has previously noted that a considerable gap persists between state-of-the-art numerical solution procedures and current practice, with adaptive methods of the kind employed here being largely confined to the field of applied mathematics rather than broader areas of contemporary research in the physical sciences [11]. In this paper, we demonstrate how static remeshing may be straightforwardly and effectively incorporated into an MOL simulation of a single-layer LED. The example chosen clearly illustrates the power of the SRM, permitting considerably improved accuracy at markedly lower computational overhead. Our approach is easily extended to more complex systems—such as injection-limited LEDs with trap sites and light-emitting electrochemical cells—as we show elsewhere [12]. The numerical procedure outlined in this paper has been designed to address a number of specific requirements: high spatial resolution for accurately modelling steep moving solution fronts; good numerical stability for handling high carrier concentrations and low (or sharply differing) electron and hole mobilities; faithful replication of temporal dynamics; and flexible and extensible program structure and good overall numerical efficiency. The procedure is found to serve well as a general purpose technique for simulating organic devices, including LEDs operating under steady-state or pulsed conditions and light-emitting electrochemical cells.

THE TRANSPORT EQUATIONS

A typical single-layer LED comprises a layer of intrinsic molecular semiconductor (typically of thickness 100 to 200 nm) sandwiched between a metallic cathode and a transparent anode such as indium tin oxide [1]. As the semiconductors are used in an undoped state, and the π–π^* energy gap is typically 2–3 eV, the LED is best viewed as a metal–insulator–metal structure. In general, the current flowing through the device will be determined by the impedances of the electrode–semiconductor interfaces and the transport characteristics of the bulk semiconductor. Two extreme situations may be considered: the injection-limited regime [13] or the space-charge-limited regime [14]. In the injection-limited case it is assumed that the impedance of the bulk semiconductor is small compared to the impedances of the electrode–semiconductor interfaces. In the space-charge-limited case, by contrast, the impedances of the electrode–semiconductor interfaces are assumed to be so low that the behaviour of the device is governed entirely by the mobility of the charge carriers in the semiconductor. In this paper we consider the space-charge-limited regime, which is typical of properly specified commercial devices for which the electrodes have been well matched to the energy bands of the semiconductor. However, as shown elsewhere, the method-of-lines framework allows for the straightforward incorporation of many additional effects, including interfacial impedances, field-dependent mobilities (via appropriate modification of Eqs. (10) and (11)) and exciton diffusion [6, 15]. The approach is readily extended to multilayered structures, without requiring substantial revision of the underlying code. In all cases use of an adaptive grid improves the efficiency of the MOL algorithm.

We assume that the semiconductor has a negligible intrinsic carrier density and is trap-free and that carrier mobilities are independent of the internal electric field. The organic

film has a thickness d, the anode is located at $x = 0$, and the cathode is at $x = d$. Neglecting interfacial impedances, the cathode and anode are assumed to supply fixed concentrations n_e^d and n_h^0 of electrons and holes respectively, with the charge densities falling to zero at the counterelectrode (i.e., $n_e^0 = 0$ and $n_h^d = 0$). The time evolution of the charge distributions is governed by Poisson's equation (1)

$$\nabla_x^2 \phi = \frac{-e}{\varepsilon}(n_h - n_e) \tag{1}$$

and the transport equations for electrons and holes,

$$\frac{\partial n_e}{\partial t} = -\nabla_x j_e - k_{eh} n_e n_h, \tag{2}$$

$$\frac{\partial n_h}{\partial t} = -\nabla_x j_h - k_{eh} n_e n_h. \tag{3}$$

The fluxes are given by

$$j_e = -\mu_e \left(\frac{kT}{e} \nabla_x n_e - n_e \nabla_x \phi \right), \tag{4}$$

$$j_h = -\mu_h \left(\frac{kT}{e} \nabla_x n_h + n_h \nabla_x \phi \right). \tag{5}$$

In these equations, ϕ is the electric potential; n, μ, and j refer to the concentrations, mobilities, and fluxes of the charge carriers respectively; and the subscripts e and h signify electrons and holes. k_{eh} is the (Langevin) electron–hole recombination rate and we have assumed that the Einstein relationship between diffusivity and mobility applies. All other symbols have their usual meanings. We stress that the transport equations employed here been chosen for illustrative purposes only and the technique may be readily applied to other systems with minimal effort.

It is helpful to recast Eqs. (2)–(5) using the dimensionless variables $\chi = x/d$, $V = -e\phi/kT$, $u_e = n_e/n_e^d$, and $u_h = n_h/n_h^0$, whereupon we obtain

$$\nabla_\chi^2 V = \frac{ed^2}{\varepsilon} \left(\frac{e}{kT} \right) \left(n_e^d u_e - n_h^0 u_h \right), \tag{6}$$

$$\frac{\partial u_e}{\partial t} = \frac{\mu_e}{d^2} \left(\frac{kT}{e} \right) \left(\nabla_\chi^2 u_e + \nabla_\chi u_e \nabla_\chi V + u_e \nabla_\chi^2 V \right) - k_{eh} n_h^0 u_e u_h, \tag{7}$$

$$\frac{\partial u_h}{\partial t} = \frac{\mu_h}{d^2} \left(\frac{kT}{e} \right) \left(\nabla_\chi^2 u_h - \nabla_\chi u_h \nabla_\chi V - u_h \nabla_\chi^2 V \right) - k_{eh} n_e^d u_e u_h. \tag{8}$$

The partial differential equations may be transformed into a series of coupled ODEs by approximating the spatial derivatives numerically. This is achieved in a straightforward manner by replacing the continuous variables $u_e(\chi, t)$, $u_h(\chi, t)$, and $V(\chi, t)$ with discrete vector expressions $\mathbf{u_e}$, $\mathbf{u_h}$, and $\mathbf{V}$ and by replacing the differential operators ∇_χ and ∇_χ^2 with finite-difference matrices D_1 and D_2 (i.e., premultiplication of $\mathbf{u_h}$ by D_1 for instance returns the first derivative of $\mathbf{u_h}$ with respect to χ). This yields

$$D_2 \mathbf{V} = \frac{ed^2}{\varepsilon} \left(\frac{e}{kT} \right) \left(n_e^d \mathbf{u_e} - n_h^0 \mathbf{u_h} \right), \tag{9}$$

$$\frac{\partial \mathbf{u_e}}{\partial t} = \frac{\mu_e}{d^2}\left(\frac{kT}{e}\right)\{D_2\mathbf{u_e} + (D_1\mathbf{u_e}) \circ (D_1\mathbf{V}) + \mathbf{u_e} \circ D_2\mathbf{V}\} - k_{eh}n_h^0\mathbf{u_e} \circ \mathbf{u_h}, \quad (10)$$

$$\frac{\partial \mathbf{u_h}}{\partial t} = \frac{\mu_h}{d^2}\left(\frac{kT}{e}\right)\{D_2\mathbf{u_h} - (D_1\mathbf{u_h}) \circ (D_1\mathbf{V}) - \mathbf{u_h} \circ D_2\mathbf{V}\} - k_{eh}n_e^d\mathbf{u_e} \circ \mathbf{u_h}, \quad (11)$$

with $\mathbf{a} \circ \mathbf{b}$ representing the element-by-element vector multiplication of $\mathbf{a}$ and $\mathbf{b}$.

The choice of an appropriate finite-difference scheme for evaluating D_1 and D_2 is somewhat problem dependent with higher order schemes offering greater accuracy at the expense of additional computational overhead for each time step. For most situations a simple three-point scheme is adequate although, for very steep moving fronts, convergence may sometimes be obtained more rapidly using higher order schemes. In this paper, we use seven-point finite-difference formulas, determined using the Lagrange polynomial method of Fornberg [16].

The MOL approach typically requires the equations to be expressed as explicit first-order differential equations with respect to time (or alternatively Eqs. (9)–(11) may be posed and subsequently solved as a mass-matrix problem). Equations (10) and (11) are already in the appropriate form, but (9) must be modified before use. Medlin *et al*. have previously reported the use of a so-called pseudo-Poisson equation, where a modified equation of the form $\frac{\partial \phi}{\partial t} = \nabla_x^2\phi + \frac{e}{\varepsilon}\{n_h - n_e\}$ is used in place of the Poisson's equation [17]. The pseudo-Poisson approach offers rapid convergence to the true steady-state solution but does not provide insight into the time evolution of the system owing to its inherent artificiality. It is also susceptible to numerical instabilities. We employ a different, and somewhat more intuitive, approach here in which (9) is differentiated with respect to time and both sides of the resultant equation are premultiplied by the inverse matrix D_2^{-1} (where $D_2D_2^{-1} = I$) to obtain.

$$\frac{\partial \mathbf{V}}{\partial t} = \frac{ed^2}{\varepsilon}\left(\frac{e}{kT}\right)D_2^{-1}\left(n_e^d\frac{\partial \mathbf{u_e}}{\partial t} - n_h^0\frac{\partial \mathbf{u_h}}{\partial t}\right). \quad (12)$$

Although D_2^{-1} may be explicitly determined, evaluating $\partial\mathbf{V}/\partial t$ in this manner is computationally inefficient because D_2 is a band-diagonal sparse matrix whereas D_2^{-1} is full. It is therefore preferable to evaluate the right-hand side of (12) in a manner which takes advantage of the sparsity of D_2. (This may be achieved for example by performing an LU decomposition of D_2 preceded by a minimum-degree preordering [18].)

Equations (10)–(12) may be integrated forward in time using an appropriate ODE integrator. Spatial discretisation of the partial differential equations results in a system of highly stiff ordinary differential equations and consequently it is necessary to employ an appropriate stiff numerical solver. Saucez *et al.* report successful use of an implicit Runge–Kutta method for many systems [19]. In this problem, we have had greater success with variable-step, variable-order backwards differentiation formulas, owing perhaps to the extreme stiffness of the differential equations. (Specifically, we employ a quasi-constant-step-size implementation in terms of backward differences of the Klopfenstein–Shampine family of numerical differentiation formulas of orders one to five [20].) We note, however, that variable-order solvers are in general less desirable for static remeshing procedures as they must be reset to first order after every remeshing process, reducing numerical efficiency. Variable-step implicit Runge–Kutta integrators do not require information about the past history of the dependent variables and are therefore usually better suited to periodic remeshing.

The remeshing algorithm is intended to locate nodes preferentially in regions where the solution is rapidly changing at the expense of coverage in quieter areas. This may be achieved simply and effectively by equidistribution of an appropriate functional. Sanz-Serna, for example, proposed a mesh algorithm to relocate mesh points at equal distances along the solution arc [21]. This represents a significant improvement over the usual equidistribution of mesh points along the spatial axis. However, as observed by Revilla, equidistribution by arc length still leads to an excessive number of nodes in regions where the solution is linear [7]. Revilla therefore proposed an alternative equidistribution scheme based on the curvature of the solution that under many circumstances leads to a more optimal distribution of grid points. Hybrid schemes may also be envisaged to allow for adequate coverage in both linear regions and those of high curvature. Saucez *et al.* have reported an extension to the approaches of Sanz-Serna and Revilla which under many circumstances offers superior performance [11, 19].

Here we use the equidistribution function proposed by Revilla which involves equidistribution of a functional $m(s)$ based on the curvature of the solution $\partial^2 s(\chi, t)/\partial \chi^2$. The equidistribution criterion we use is

$$\int_{\chi_{i-1}}^{\chi_i} m(s(\chi, t))\, d\chi = \int_{\chi_{i-1}}^{\chi_i} \left(\alpha + \left\| \frac{\partial^2 s(\chi, t)}{\partial \chi^2} \right\|\right)^{1/2} d\chi = \text{constant}, \tag{13}$$

where s is the solution vector and α is a problem-dependent parameter, and is discussed more completely in the Appendix and Ref. [7].

In the case of the LED there are three possible solution curves we could consider for performing the equidistribution process: $n_e(x)$, $n_h(x)$, and $\phi(x)$. The electric potential—or its dimensionless equivalent $V(\chi)$—is the obvious choice here as its curvature depends directly on the changing concentrations of electrons *and* holes. Moreover, given the integral relationship between the potential and the charge densities, $\phi(x)$ is typically the smoothest of the three functions and is therefore best suited to the remeshing algorithm. Following the approach of Adjerid and Flaherty [22], the time integration is halted and the spatial grid is updated periodically after a fixed number *nsteps* of integration steps. Since the time increments used by the ODE solver will become smaller when the solution is changing rapidly, this approach ensures that grid updates occur most frequently during periods of intense activity.

SOLUTION OF THE TRANSPORT EQUATIONS

In this paper, we concentrate primarily on the numerical properties of the fixed-grid and adaptive grid algorithms, and we defer discussion of the physical significance of the results to a separate paper [12]. Incorporation of a remeshing algorithm into the MOL procedure leads to substantial improvements in numerical efficiency. This is primarily because the number of grid points may be substantially reduced for any prescribed level of accuracy. Sanz-Serna and Christie [21] and Revilla [7] have reported that the number of nodes may be reduced by up to a factor of 12 according to the problem under study and the choice of equidistribution function. It should be stressed that, since computational overhead increases superlinearly with the number of nodes, the ability to reduce grid size leads to very substantial savings in computing time.

There are two important sources of error in MOL algorithms: errors associated with the time integration and discretisation errors arising from the use of a finite grid. To ensure that spatial errors dominated the results reported here, time integration was performed using strict relative and absolute error tolerances of 10^{-7}. It is desirable to compare the numerical results with known analytical solutions, but this is not generally possible owing to the intractability of the coupled differential equations. An *exact* analytical solution has been reported by Mott and Gurney for the specific case of Ohmic injection of a single carrier type into an insulator, neglecting diffusion, in which case the electric potential varies as $\lfloor (Bx + C)^{3/2} - C^{3/2} \rfloor$, where x is the distance from the injecting contact and B and C are constants that depend on the current density and the device parameters [14]. This (nonphysical) diffusion-free situation is difficult to simulate numerically owing to the absence of diffusion effects that would otherwise broaden the solution fronts, and rigorous evaluation of numerical errors is not therefore possible even for this one exactly soluble situation. It is however possible to reduce the diffusivities of the charge carriers to relatively small levels without adversely affecting numerical convergence by reducing the notional temperature. Cautious comparison between the numerical and analytical results is then possible, although discrepancies between the two solutions are more likely to arise from genuine physical differences between the systems studied than errors in the numerical simulation.

The simulations in Figs. 1–3 were carried out at a notional temperature of 3 K corresponding to diffusivities 100 times smaller than their room temperature values. The remaining parameters—chosen to ensure steep solution profiles at the injecting contact—were

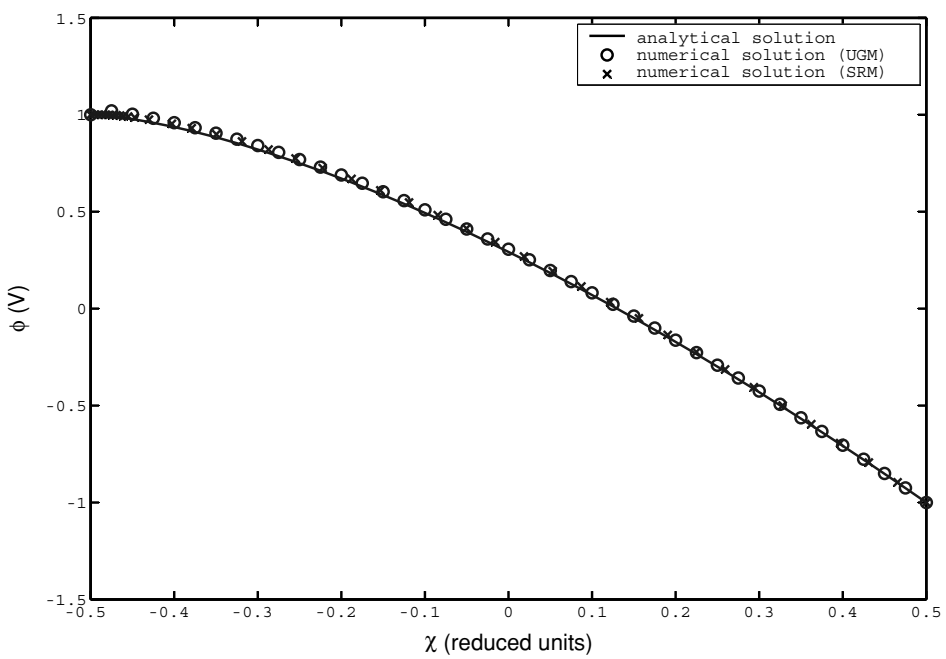

FIG. 1. Numerical simulations of the steady-state electric potential in LEDs operating in the unipolar space-charge-limited regime, determined using 41-node uniform and adaptive grids. Parameters for the unipolar problem were $n_h^0 = 10^{23}$ m^{-3}, $\mu_h = 10^{-7}$ m^2 V^{-1} s^{-1}, $\phi_0 - \phi_d = 2$ V, $\varepsilon_r = 3.4$, and $d = 1$ μm. The analytical solution (assuming zero diffusion) is shown for reference.

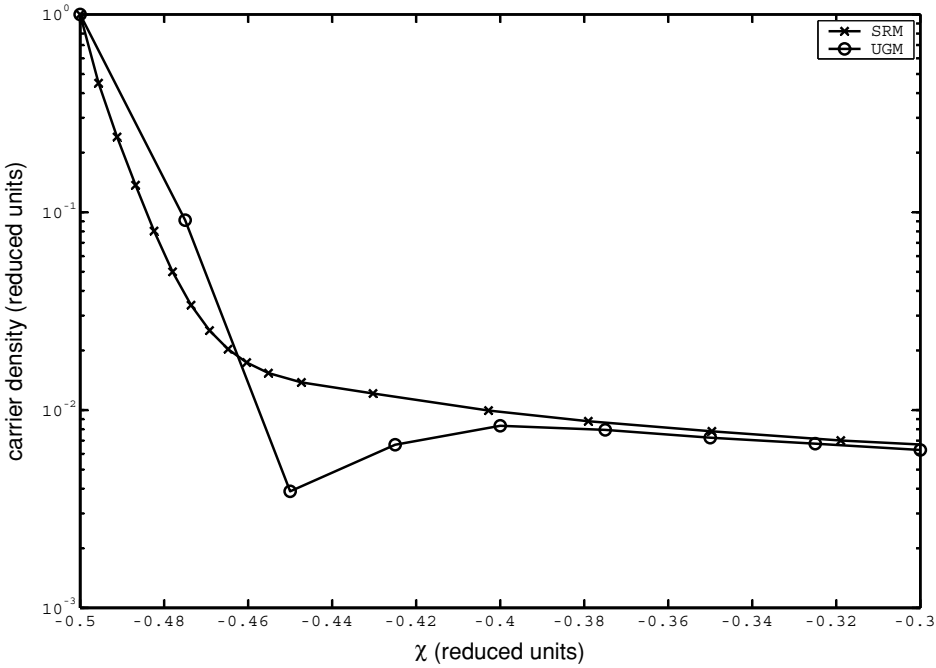

FIG. 2. Numerical simulations of the steady-state hole distribution in LEDs operating in the unipolar space-charge-limited regime, determined using 41-node uniform and adaptive grids. The UGM solution displays an unphysical discontinuity in the first derivative. The SRM solution varies smoothly with position and is consistent with physical expectation. The linearity of the SRM solution in the immediate vicinity of the electrode suggests that a more accurate solution might be obtained by increasing the number of grid points. The same parameters were used as for Fig. 1.

$n_h^0 = 10^{23}\,\mathrm{m}^{-3}$, $\mu_h = 10^{-7}\,\mathrm{m}^2\,\mathrm{V}^{-1}\,\mathrm{s}^{-1}$, $\phi_0 - \phi_d = 2\mathrm{V}$, $\varepsilon_\mathrm{r} = 3.4$, and $d = 1\ \mu\mathrm{m}$. Figure 1 shows solutions for the steady-state electric potential obtained using uniform and adaptive grids with 41 nodes. In each case a reasonable approximation of the analytical solution for the electric potential is obtained, with the UGM having an average root-mean squared deviation from the analytical solution of 0.9%, and the SRM showing a deviation of 0.6%. The small deviations obtained confirm—at least in a semiquantitative sense—the validity of the MOL approach in both cases, but they do not in themselves suggest there is a major advantage to using spatial remeshing in this instance. This, however, is to be expected since the profile of the electric potential generally varies smoothly and slowly in space. The steady-state charge density on the other hand changes extremely rapidly in the vicinity of the injecting electrode and therefore represents a more exacting numerical challenge. Figure 2 shows the profile of holes close to the anode determined using the same 41-node uniform and adaptive grids. The UGM solution is clearly unsatisfactory, exhibiting an unphysical discontinuity in the first derivative. The SRM solution by contrast varies fairly smoothly with distance away from the electrode, which is consistent with physical expectation. The linear nature of the 41-node SRM solution in the immediate vicinity of the electrode suggests that a superior solution might be obtained by increasing the number of nodes. Figure 3 shows the profiles of holes determined using uniform and spatial grids with 101 nodes. The 101-node SRM solution varies smoothly with distance from the electrode, albeit slightly more sharply than in Fig. 2. Its profile was not found to alter noticeably with larger numbers

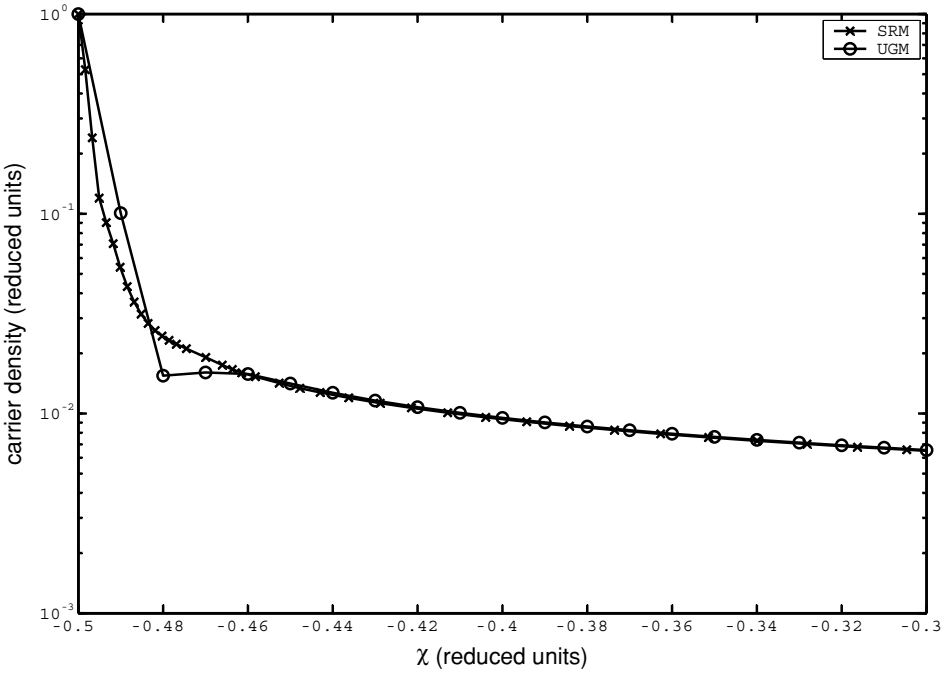

FIG. 3. Numerical simulations of the steady-state hole distribution in LEDs operating in the unipolar space-charge-limited regime, determined using 101-node uniform and adaptive grids. The 101-node UGM solution still displays an unphysical discontinuity in the first derivative and is inferior even to the 41-node SRM solution. The 101-node SRM solution varies smoothly with position and is not found to improve significantly when the number of nodes is increased. The same parameters were used as for Fig. 1.

of grid points, confirming the adequacy of 101-node remeshing for this particular problem. The 101-node UGM solution by contrast still displays an unphysical discontinuity in the first derivative, implying the need for yet more grid points. In fact, to obtain an acceptable solution using the UGM, it would be necessary to use at least 400 nodes (corresponding to 2.5-nm spatial resolution), which in practice was not possible as the underlying ODE solver would not converge for a problem of this size. Figure 4 shows the steady-state hole profiles for a bipolar device operating at 3 K using the same parameters as before to ensure steep solution profiles, and additionally $n_e^d = 10^{23}\,\mathrm{m}^{-3}$ and $\mu_e = 10^{-7}\,\mathrm{m}^2\,\mathrm{V}^{-1}\,\mathrm{s}^{-1}$. (The profile of the electron distribution, which is not shown, mirrors that of the hole distribution for the parameters selected.) The solutions were determined using 151-node uniform and adaptive grids. The SRM is again found to deliver far superior solutions by concentrating nodes in regions close to the anode and the cathode at the expense of coverage in the bulk of the device.

The ability to limit the number of nodes and place them in optimal locations leads to substantial improvements in the efficiency of the MOL algorithm. Table I presents computational statistics for the fixed and adaptive grids. In spite of the additional overhead associated with periodically halting the time integration and assigning new mesh points, for larger grids, adaptation usually hastens convergence to the steady state whilst *simultaneously* offering superior spatial resolution (in the regions where it is needed). The performance of the UGM can in principle be improved to an arbitrary extent by increasing the number of nodes. However, in practice, as can be seen from the illustrative CPU statistics, relatively

TABLE I

Computational Statistics for Simulations of Single-Layer LEDs Operating in the Space-Charge-Limited Regime, Determined Using a Fixed Uniform Grid (×) and Static Spatial Remeshing (✓)

Simulation	Nodes	Regridding	STEPS (successful)	FSTEPS (failed)	FNS	JACS	CPU (s)
Unipolar injection	41	×	825	75	1722	2	11
		✓	882	49	2205	7	14
	101	×	6791	122	28994	50	641
		✓	5420	84	15058	27	343
	151	×	3453	916	164058	344	3097
		✓	8379	248	61918	112	1661
	201	×	14632	1168	332894	500	11435
		✓	11472	649	165980	246	5976
Bipolar injection	151	×	10205	814	170851	342	3912
		✓	8012	202	54132	97	1686

Note. STEPS is the number of successful time steps required to complete the simulation; FSTEPS is the number of failed steps; FNS is the number of function evaluations; JACS is the number of Jacobian evaluations; and CPU, which is given for information only, is the computational time using a 750-MHz Athlon processor. For larger grid sizes, adaptive remeshing is seen to hasten numerical convergence. Parameters for the unipolar problem were $n_h^0 = 10^{23}\ \mathrm{m}^{-3}$, $\mu_h = 10^{-7}\ \mathrm{m}^2\ \mathrm{V}^{-1}\ \mathrm{s}^{-1}$, $\phi_0 - \phi_d = 2\,\mathrm{V}$, $\varepsilon_r = 3.4$, and $d = 1\,\mu\mathrm{m}$. The same parameters were used for the bipolar problem with $n_e^d = 10^{23}\ \mathrm{m}^{-3}$ and $\mu_e = 10^{-7}\ \mathrm{m}^2\ \mathrm{V}^{-1}\ \mathrm{s}^{-1}$.

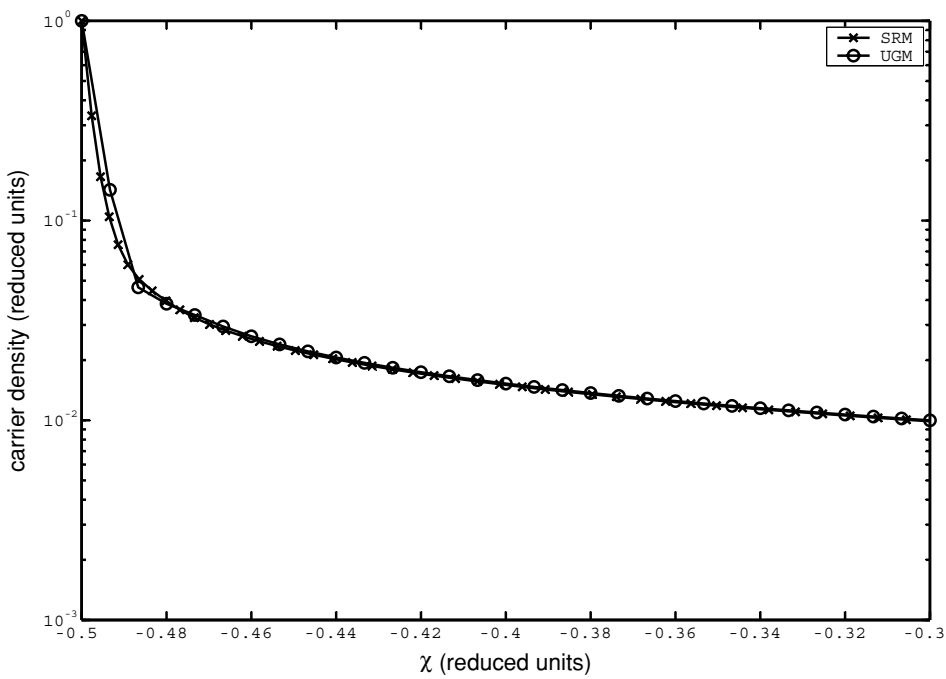

FIG. 4. Numerical simulations of the steady-state hole distribution in LEDs operating in the bipolar space-charge-limited regime, determined using 151-node uniform and adaptive grids. The SRM solution offers higher spatial resolution in the regions of interest. The same parameters were used as for Fig. 1 with $n_e^d = 10^{23}\ \mathrm{m}^{-3}$ and $\mu_e = 10^{-7}\ \mathrm{m}^2\ \mathrm{V}^{-1}\ \mathrm{s}^{-1}$.

small increases in grid size can lead to exceptionally large increases in convergence time (and excessive memory requirements, which may in turn cause the underlying ODE solver to fail). Spatial remeshing to some extent circumvents this problem by (i) reducing the number of nodes required to obtain a satisfactory solution and (ii) hastening numerical convergence for that particular number of grid points. In the unipolar space-charge-limited regime considered here, for example, the superior 101-node steady-state SRM solution was obtained approximately 20 times "faster" than the 201-node UGM solution. Grid adaptation therefore represents a very important technique for the successful numerical investigation of organic devices. Moreover, as we shall show in a later paper, for simulating devices such as light-emitting electrochemical cells in which extremely high fields exist close to each interface, spatial remeshing is *absolutely* necessary if an answer is to be obtained at all.

To some extent the effectiveness of fixed-grid algorithms may be improved by preferentially locating nodes in areas of known activity. This, however, requires *a priori* knowledge of the solution, obtained (at a cost), for example, by first solving the problem using a uniform grid. Because the SRM adapts to the evolving system of equations, no *a priori* knowledge of the solution curve is required. It should also be noted that for certain problems, such as the light-emitting electrochemical cell [8–10], the profile of the solution changes radically with time. In such cases, preferential deployment of fixed grid points in locations determined by the final profile of the (steady-state) solution may actually reduce efficiency by hindering the evolution of the equations at earlier times. This problem does not arise with grid adaptation as the nodes are regularly relocated in spatial regions of high activity.

CONCLUSION

We have used a simple but effective method-of-lines approach for solving the highly nonlinear coupled differential equations which govern the behaviour of organic space-charge-limited light-emitting diodes. Use of an adaptive mesh allows the number of nodes to be reduced substantially for any prescribed level of accuracy, leading to considerable increases in numerical efficiency. The static remeshing algorithm we employ here, based on the approach of Revilla [7], requires no *a priori* knowledge of the solution curve and hastens conversion to the steady-state solution. The algorithm is independent of the system of equations under study and may be applied to other problems without change. Importantly, and unlike dynamic remeshing algorithms, it does not give rise to ill-conditioned sets of differential equations. Overall, the procedure is found to offer a general purpose and numerically efficient approach to simulating a wide range or organic devices.

APPENDIX

The remeshing algorithm is invoked after the time integrator has completed a total of *nsteps* iterations. As discussed previously, the vector expression $\underline{V}$ is first used to calculate the equidistribution function defined by

$$I(\chi', t) = \int_0^{\chi'} \left(\alpha + \left\| \frac{\partial^2 V(\chi, t)}{\partial \chi^2} \right\| \right)^{1/2} d\chi. \tag{A1}$$

It is necessary to specify two parameters in the equidistribution function, α and β: α modifies the relative importance of values of the dependent and independent variables; and β prevents excessive clustering of nodes (which in turn causes numerical difficulties) by placing a ceiling on overly high values of the second derivative. If the value of $\partial^2 V(\chi, t)/\partial \chi^2$ exceeds β anywhere along the solution arc, $\partial^2 V(\chi, t)/\partial \chi^2$ is reduced to a value of β before evaluating (A1). For all situations reported here, α and β were set to the empirically determined values of 1 and 60 respectively.

The form of the functional in (A1) is justified fully in Ref. [7] so we provide only a brief explanation here. In short, the integrand of (A1) involves the second derivative of the solution $V(\chi, t)$ and is therefore related to its curvature. $I(\chi', t)$ may be interpreted as a cumulative measure of the solution curvature in the range $0 \leq \chi \leq \chi'$. According to the equidistribution principle, the locations of the new data points should be chosen to ensure that $I(\chi)$ increases by the same amount in moving between successive nodes; this is stated mathematically as

$$\int_{\chi_{i-1}}^{\chi_i} \left(\alpha + \left\| \frac{\partial^2 V(\chi, t)}{\partial \chi^2} \right\| \right)^{1/2} d\chi = \text{constant} = \left(\frac{I(1, t)}{N - 1} \right). \tag{A2}$$

Combining (A1) and (A2) we obtain

$$I\left(\chi_i^{\text{new}}, t\right) = \left(\frac{(i - 1) \times I(1, t)}{N - 1} \right), \tag{A3}$$

and finally

$$\chi_1^{\text{new}}, \chi_2^{\text{new}}, \ldots, \chi_{N-1}^{\text{new}}, \chi_N^{\text{new}} = 0, I^{-1}\left(\frac{1 \times I(1, t)}{N - 1} \right), \ldots, I^{-1}\left(\frac{(N - 2) \times I(1, t)}{N - 1} \right), 1 \tag{A4}$$

where N is the number of nodes and $I^{-1}[I(\chi')] = \chi'$, which provides the locations of the new nodes.

After determining the spatial locations of the new nodes, we may obtain estimates of the corresponding values of V, u_e, and u_h using Lagrange polynomial interpolation [16]. The time integration is then restarted and continues until a further *nsteps* iterations have been completed, following which the remeshing algorithm is again invoked.

ACKNOWLEDGMENTS

We thank Drs. Ahrash Daneshvar and Jenny Nelson for useful comments and suggestions on the manuscript.

REFERENCES

1. R. H. Friend, R. W. Gymer, A. B. Holmes, J. H. Burroughes, R. N. Marks, C. Taliani, D. D. C. Bradley, D. A. Dos Santos, J. L. Bredas, M. Logdlund, and W. R. Salaneck, Electroluminescence in conjugated polymers, *Nature* **397**(6715), 121 (1999).
2. P. A. Torpey, Double-carrier injection and recombination in insulators, including diffusion effects, *J. Appl. Phys.* **56**(8), 2284 (1984).

3. N. Tessler, Transport and optical modeling of organic light-emitting diodes, *Appl. Phys. Lett.* **77**(12), 1897 (2000).
4. H. Bassler, Injection, transport and recombination of charge carriers in organic light-emitting diodes, *Polymers Adv. Technol.* **9**(7), 402 (1998).
5. D. J. Pinner, R. H. Friend, and N. Tessler, Time-resolved transport in conjugated polymers, *Synth. Met.* **111**, 257 (2000).
6. G. G. Malliaras and J. C. Scott, Numerical simulations of the electrical characteristics and the efficiencies of single-layer organic light emitting diodes, *J. Appl. Phys.* **85**(10), 7426 (1999).
7. M. A. Revilla, Simple time and space adaptation in one-dimensional evolutionary partial-differential equations, *Int. J. Numer. Methods Eng.* **23**(12), 2263 (1986).
8. Q. B. Pei, Y. Yang, G. Yu, C. Zhang, and A. J. Heeger, Polymer light-emitting electrochemical-cells, *Science* **269**(5227), 1086 (1995).
9. J. C. deMello, N. Tessler, S. C. Graham, and R. H. Friend, Ionic space-charge effects in polymer light-emitting diodes, *Phys. Rev. B* **57**(20), 12951 (1998).
10. J. C. deMello, J. J. M. Halls, S. C. Graham, N. Tessler, and R. H. Friend, Electric field distribution in polymer light-emitting electrochemical cells, *Phys. Rev. Lett.* **85**(2), 421 (2000).
11. A. V. Wouwer, P. Saucez, and W. E. Schiesser, Some user-oriented comparisons of adaptive grid methods for partial differential equations in one space dimension, *Appl. Numer. Math.* **26**(1–2), 49 (1998).
12. J. C. deMello, *Interfacial Feedback Dynamics in Polymer Light-Emitting Electrochemical Cells*, unpublished.
13. S. M. Sze, *Physics of Semiconductor Devices* (Wiley, New York, 1981).
14. N. F. Mott and R. W. Gurney, *Electronic Processes in Ionic Crystals* (Oxford Univ. Press, London, 1940).
15. N. Tessler, D. J. Pinner, and R. H. Friend, Semiconductor device model applied to electrically pulsed polymer LEDs, *Synth. Met.* **111**, 269 (2000).
16. B. Fornberg, Generation of finite-difference formulas on arbitrarily spaced grids, *Math. Comput.* **51**(184), 699 (1988).
17. A. J. Medlin, C. A. J. Fletcher, and R. Morrow, A pseudotransient approach to steady state solution of electric field-space charge coupled problems, *J. Electrostat.* **43**(1), 39 (1998).
18. W. H. Press, S. A. Teukolsky, W. T. Vetterling, and B. P. Flannery, *Numerical Recipes in C* (Cambridge Univ. Press, Cambridge, UK, 1992).
19. P. Saucez, A. VandeWouwer, and W. E. Schiesser, Same observations on a static spatial remeshing method based on equidistribution principles, *J. Comput. Phys.* **128**, 274 (1996).
20. L. F. Shampine and M. W. Reichelt, The MATLAB ODE suite, *SIAM J. Sci. Comput.* **18**(1), 1 (1997).
21. J. M. Sanz-Serna and I. Christie, A simple adaptive technique for nonlinear-wave problems, *J. Comput. Phys.* **67**, 348 (1986).
22. S. Adjerid and J. E. Flaherty, A moving finite-element method with error estimation and refinement for one-dimensional time-dependent partial-differential equations. *SIAM J. Numer. Anal.* **23**(4), 778 (1986).